J Biosci (2019) 44:105
DOI: 10.1007/s12038-019-9921-3

Biosensor design using an electroactive label-based aptamer to detect bisphenol A in serum samples

Maryam Nazari[1,2], Soheila Kashanian[3,4]*, Ronak Rafipour[5] and Kobra Omidfar[1,6]

[1]*Biosensor Research Center, Endocrinology and Metabolism Molecular-Cellular Sciences Institute, Tehran University of Medical Sciences, Tehran, Iran*

[2]*Faculty of Chemistry, Razi University, Kermanshah, Iran*

[3]*Faculty of Chemistry, Sensor and Biosensor Research Center (SBRC) & Nanoscience and Nanotechnology Research Center (NNRC), Razi University, Kermanshah, Iran*

[4]*Nano Drug Delivery Research Center, Kermanshah University of Medical Science, Kermanshah, Iran*

[5]*Department of Chemistry, Kermanshah Branch, Islamic Azad University, Kermanshah, Iran*

[6]*Endocrine and Metabolism Research Center, Endocrinology and Metabolism Research Institute, Tehran University of Medical Sciences, P.O. Box 14395/1179, Tehran, Iran*

**Corresponding author (Email, kashanian_s@yahoo.com)*

MS received 8 March 2019; accepted 14 June 2019; published online 16 August 2019

A new and simple procedure was applied to detect bisphenol A (BPA) based on a BPA aptamer and its complementary strand (Comp. Str.). An electrode was modified with a mixture of carboxylated multiwalled carbon nanotubes and chitosan. The Comp. Str. was immobilized on a modified-glassy carbon electrode (GCE) surface via covalent binding. After the incubation of the aptamer with the electrode surface, it could interact with the Comp. Str. In the presence of BPA, its aptamer will interact with the analyte, resulting in some changes in the configuration and leading to separation from the electrode surface. Due to the attached ferrocene (Fc) group on the 5′ head of the aptamer, the redox current of Fc has reduced. This aptasensor can sense the level of BPA in the linear range of 0.2–2 nM, with a limit of detection of 0.38 nM and a sensitivity of 24.51 μA/nM. The proposed aptasensor showed great reliability and selectivity. The acceptable selectivity is due to the specificity of BPA binding to its aptamer. The serum sample was used as a real sample; the aptasensor was able to effectively recover the spiked BPA amounts. It can on-site monitor the BPA in serum samples with acceptable recoveries.

Keywords. Aptasensor; bisphenol A; chitosan; ferrocene; multiwalled carbon nanotubes

1. Introduction

One of the important molecules for the production of epoxy resins and polycarbonate plastics is bisphenol A (BPA), which is used in food-storage components, ovenware and packaging materials (Xue *et al.* 2013; Yan *et al.* 2018). It is known to be a common pollutant, hazardous and toxic to the health of human and animals; also, it reduces the function of the immune system and fertility and causes different cancers after being exposed for a long time (Maiolini *et al.* 2014; Sheikh *et al.* 2017). BPA is able to bind to estrogen receptors due to its similar structure to endocrine hormones (Zimmers *et al.* 2014). The exposure to this endocrine disruptor from food contact materials was estimated by the Food and Drug Administration (FDA) to be ∼0.185 and 2.42 μg/kg body weight per day for adults and infants, respectively (FDA 2014). The use of BPA was banned in baby bottles in 2010 and 2011 in Canada and China, respectively. Also, in all European Union countries the use of BPA was prohibited in baby bottles from January 2011 (Zehani *et al.* 2015). The current level of tolerable daily intake of BPA was recommended to be 4 μg/kg of body weight per day by the European Food Safety Authority (EFSA 2015). BPA has the ability to act as the mimic of the 17-β estradiol hormone in structure and function; it can be connected to the estrogen receptors and can affect the health (Steinmetz *et al.* 1997; Sekar *et al.* 2016). BPA determination is difficult due to the weak response of common optical methods and electrochemical sensors and low sensitivity of their interfering substance effects. It is necessary to develop a sensitive and simple technique. There is a crucial

need to develop rapid, selective, sensitive, quantitative and economic analytical approaches for accurate determination of BPA in numerous aqueous food and biological serum samples to evaluate BPA exposure. Various analytical approaches have been stated for BPA detection including liquid and gas chromatography (Cunha *et al.* 2015; Farajzadeh *et al.* 2015; Rocha *et al.* 2016; Filippou *et al.* 2017), enzyme-linked immunosorbent assay (Ohkuma *et al.* 2002; Kubo *et al.* 2014; Miao *et al.* 2014), flow injection chemiluminescence (Cao *et al.* 2014) and fluorimetry (Liu *et al.* 2016). These methods can propose a good accuracy and sensitivity, but they have some disadvantages such as complicated procedures, time consuming and expensive instrumentation; therefore, their applications are restricted (Mei *et al.* 2013; He *et al.* 2017). Furthermore, some electrochemical procedures have been advanced for the detection of BPA by construction of chemically reformed electrodes; however, their disadvantage is suffering from a moderate selectivity. The use of graphene (Zhou *et al.* 2016), polymers (Kazane *et al.* 2016), gold nanoparticles (AuNPs) (Zhang *et al.* 2016) and carbon nanotubes (Beiranvand *et al.* 2017) results in improving the detection limit, linear range and sensitivity. Biosensors show miniaturization, high sensitivity and are of low cost. Immobilization of biomolecules including peptides (Yang *et al.* 2014), antibodies (Wang *et al.* 2014; Peng *et al.* 2018), estrogen receptors (Salehi *et al.* 2018) and aptamers (Deiminiat *et al.* 2017; Ma *et al.* 2017) has been achieved to obtain high sensitivity and selectivity of BPA detection devices. Aptamers are RNA or DNA (single-stranded) sequences and can be designated and chosen *in vitro* by systematic evolution of ligands by exponential enrichment. They have high affinity and specificity for numerous molecules, ranging from huge molecules such as proteins to small molecules (Darmostuk *et al.* 2015). Their affinity for the target molecules is similar to or more than antibodies' affinity; in addition, the aptamer production does not need an immune response. The other advantages include reusability, thermal stability and denaturation resistance. Also, the modification of aptamers is easy (Huang *et al.* 2015). The first selection of an anti-BPA aptamer was reported in 2011 (Jo *et al.* 2011); many optical and electrochemical aptasensors based on this anti-BPA aptamer have been reported (Zhang *et al.* 2016; Feng *et al.* 2016; Beiranvand and Azadbakht 2017; Lv *et al.* 2018). Zhou *et al.* modified the glassy carbon electrode (GCE) by a nanocomposite of dotted-graphene films and AuNPs for immobilization of the anti-BPA aptamer and detection of BPA in milk with a limit of detection (LOD) of 5 nM (Zhou *et al.* 2014). Yu *et al.* fabricated an aptasensor based on the electrochemical approach of triple-signaling to sense very low-BPA concentrations with an LOD of 37 pg/mL in tap water (Yu *et al.* 2016).

In this study, a novel selective and sensitive electrochemical aptasensor was developed based on the oxidation and reduction of the ferrocene (Fc) group at the 5′ end of aptamer as a redox probe for BPA detection. The BPA aptamer can interact with its complementary strand (Comp. Str.), causing Fc to be near the electrode surface in the absence of BPA. When BPA is present, it interacts with the BPA aptamer leading to conformational changes of the BPA aptamer and separation of the Fc group from the electrode; consequently, the redox current was reduced. The proposed aptasensor was applied to detect BPA in the serum sample.

2. Experimental

2.1 *Reagents*

The synthetic sequence of the BPA aptamer which has been reported by Jo and his colleagues is as follows: 5′-(Fc)-$(CH_2)_6$-CCG GTG GGT GGT CAG GTG GGA TAG CGT TCC GCG TAT GGC CCA GCG CAT CAC GGG TTC GCA CCA-3′. The BPA aptamer and its Comp. Str. were synthesized by Bioron Diagnostics GmbH (Germany). Its oligonucleotide sequence is as follows: 5′-CCG GTG GG ATG CGC TGG ATA CGC GGA ACG CTA TCC CAC CTG ACC ACC CAC CGG $(CH_2)_6$-(NH_2)-3′. The stock solutions of the aptamer and complementary DNA were prepared using deionized-distilled water and stored in a refrigerator. Carboxylated multiwalled carbon nanotubes (MWCNTs-COOH) were purchased from US Research Nanomaterials, USA. N-(3-Dimethylaminopropyl)-N′-ethylcarbodiimide (EDC) and N-hydroxysulfosuccinimide (NHS) were bought from Sigma-Aldrich. Chitosan (CHIT) and BPA were obtained from Sigma-Aldrich (USA) and Asia Chem., respectively. All other materials were purchased from Merck, and the solutions were prepared using deionized forth-distilled water. Two electrolyte solutions were used in electrochemical experiments: phosphate-buffered saline (PBS, 0.1 M) and a solution comprised of $[Fe(CN)_6]^{3-/4-}$ (5 mM) and KCl (0.1 M).

2.2 *Instrumentation*

Field-emission scanning electron microscopy (FESEM) was carried out by using a Mira3TESCAN-XMU scanning electron microscope. The electrochemical experiments were carried out using a Sama500 and Metrohm (NOVA software) Autolabs linked to a conventional cell used for electrochemical impedance spectroscopy (EIS) and voltammetry measurements, respectively. Three-electrodes, a platinum wire, a saturated Ag/AgCl electrode and a GCE, were utilized as the counter, reference and working electrodes, respectively.

2.3 *Synthesizing the nanocomposite of MWCNTs-COOH and CHIT*

The nanocomposite of MWCNTs-COOH and CHIT was prepared as reported by Rafipour *et al.* (2017). Briefly, a CHIT solution (1.0% (m/v)) was prepared using 10 mg of

CHIT by dissolving it in 1 mL of acetic acid (1.0% (v/v)) solution; then it was stirred for 3 h at 25°C until completion of dissolution. For preparation of a mixture of MWCNTs-COOH in CHIT solution with the concentration of 1.0% (m/v), 1 mg of MWCNTs-COOH was dispersed in 100 μL of CHIT solution and sonicated for 5 h. The prepared nanocomposite suspension was kept at 4°C.

2.4 *Fabrication of aptasensor based on the MWCNTs-COOH/CHIT nanocomposite*

Before GCE modification, it was polished using an alumina slurry (0.05 μm), rinsed with forth-distilled water and then allowed to dry. After this, 7.0 μL of MWCNTs-COOH/CHIT nanocomposite suspension was added dropwise onto the GCE surface and dried at 25°C. Then, 7 μL of PBS (pH 7.0) was added dropwise onto the electrode surface and left to dry for 45 min; this step was repeated again. After this step, the mixture of EDC and NHS (with the concentration of 0.5% m/v for both) was used to activate the carboxyl groups of MWCNTs-COOH for complementary DNA immobilization. It was immobilized onto the surface of the modified GCE by adding 4 μL of its solution (200 μM) to the electrode surface. After drying, 8 μL of BPA aptamer solution (100 μM) was added dropwise onto the electrode surface. Finally, the prepared electrode was washed with distilled water and dried. In subsequent studies, the modified GCE was used as an aptasensor for BPA detection in PBS and serum samples.

2.5 *Electrochemical experiments*

The stock solutions of BPA were prepared in dimethyl sulfoxide at a concentration of 10^{-2} M and kept in a refrigerator at 4°C. PBS (pH 7.0) was used for the preparation of diluted-BPA fresh solutions; these solutions were used to investigate BPA and its aptamer interactions. The electrochemical experiments were carried out in a solution comprised of KCl (0.1 M) and $K_3[Fe(CN)_6]/K_4[Fe(CN)_6]$ (5 mM) redox pair. Voltammetry techniques (differential pulse voltammetry (DPV) and cyclic voltammetry (CV)) were used within the potential range of -0.5 to 0.8 V. EIS was carried out at the amplitude of 0.01 V, applied potential of 0.20 V and in the frequency ranging from 0.1 to 30,000 Hz. All of the electrochemical experiments were performed at 25°C.

2.6 *Serum sample preparation*

Blood samples were collected from the Imam Reza hospital in Kermanshah. After clotting of samples, they were centrifuged for 15 min at 2000 rpm under 4°C. The same volume of acetonitrile was added to the serum sample to clot serum proteins. The serum sample was further diluted in PBS (pH 7.0). To test the matrix effect of serum, several volumes of BPA at 1 μM in PBS were spiked in diluted human-serum samples.

3. Results

3.1 *Aptasensor characterization using FESEM and energy-dispersive X-ray spectroscopy*

The morphology of the modified electrodes was characterized by FESEM. Figure 1A shows a homogeneously spread layer of the MWCNTs-COOH/CHIT mixture and a porous reticular formation at the GCE surface. Figure 1B presents the FESEM image of the modified-electrode surface after the introduction of the MWCNTs-COOH/CHIT mixture modified with a Comp. Str. and Comp. Str./aptamer.

3.2 *Aptasensor electrochemical characterization*

The study on the interface properties of the surface-modified electrodes can be conducted using the EIS technique. It encompasses the important parameters such as the Warburg impedance (Z_W), resistance of the solution (R_s) and electron-transfer resistance (R_{et}) which are related to the diffusion contribution. The semicircular portion diameter is used for the estimation of the R_{et} value. Figure 2A shows the change in electrode impedance after each alteration and confirms our successful electrode fabrication of the sensing interface. According to figure 2A, the bare GCE showed the largest semicircle and R_{et} (1.85 kΩ). Due to the improvement of electron transfer, the R_{et} value decreased for MWCNTs-COOH,CHIT/GCE compared with that of the bare GCE which was obtained to be 72.1 Ω. Also, R_{et} were calculated for Comp. Str./MWCNTs-COOH,CHIT/GCE and aptamer/Comp. Str./MWCNTs-COOH,CHIT/GCE, which were obtained to be 790 and 154 Ω, respectively. The Nyquist plot circuit of the modified GCEs is [R(Q[RQ])].

Investigation of the presence and function of each component on the GCE surface was performed using CV. CVs of various modified electrodes were recorded in the electrolyte solution comprising KCl and $[Fe(CN)6]^{3-/4-}$. According to figure 2B, the MWCNTs-COOH,CHIT/GCE has a pair of strong redox peaks.

According to equation (1), the surface area of GCE, MWCNTs-COOH,CHIT/GCE and aptamer/Comp. Str./MWCNTs-COOH,CHIT/GCE was calculated to be 0.05, 0.70 and 3.94 cm^2, respectively. The number of electrons (n) and diffusion coefficient (D) were considered to be 1 and 7.6 $\times 10^{-6}$ cm^2/s for the redox reaction of $[Fe(CN)_6]^{3-/4-}$. C, v and A are the concentration of $K_3[Fe(CN)_6]$, scan rate and the electrode area (cm^2), respectively:

$$I_p = \left(2.69 \times 10^5\right) n^{3/2} A D^{1/2} C v^{1/2} \quad (1)$$

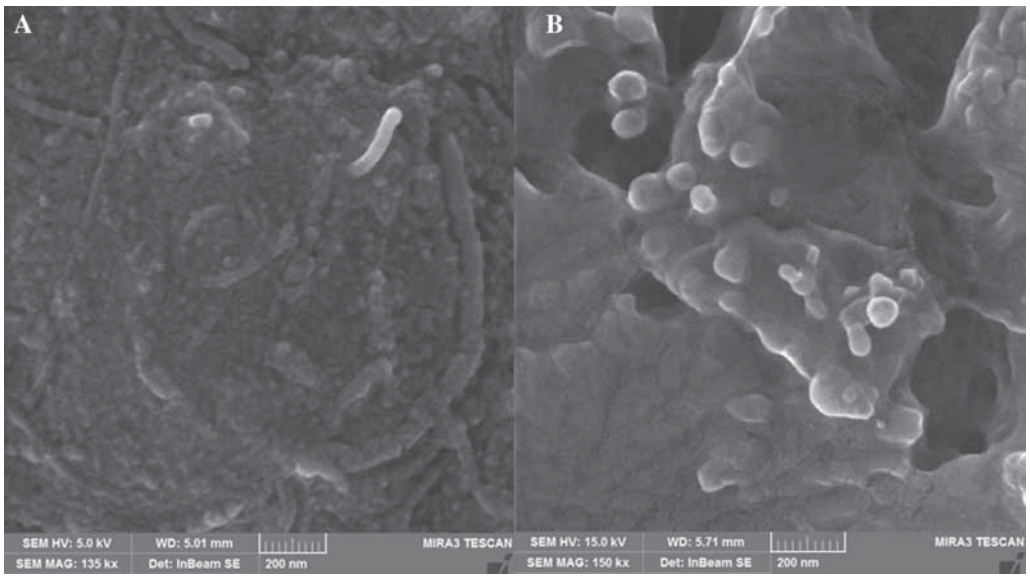

Figure 1. Typical FESEM images of MWCNTs-COOH,CHIT/GCE (**A**) and aptamer/Comp. Str./MWCNTs-COOH,CHIT/GCE (**B**).

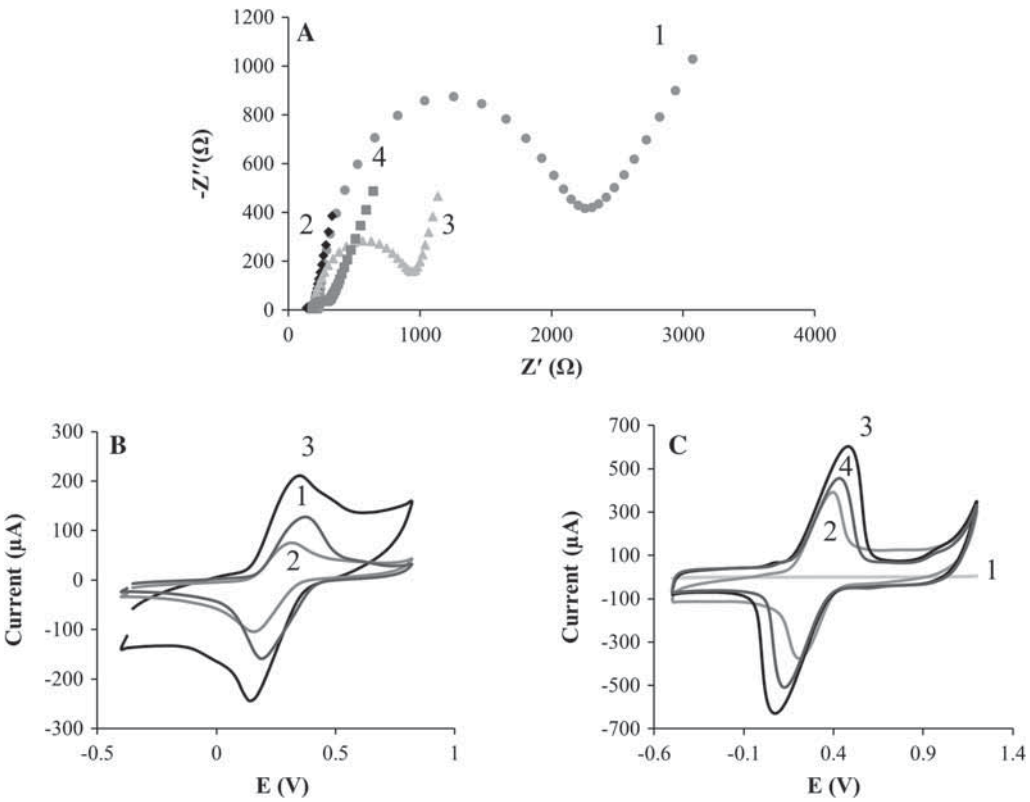

Figure 2. (**A**) Illustration of the corresponding Nyquist plots in 0.1 M KCl solution containing 5.0 mM $Fe(CN)_6^{3-/4-}$ in the frequency range of 10 kHz–0.1 Hz: bare GCE (curve 1), MWCNTs-COOH,CHIT/GCE (curve 2), Comp. Str./MWCNTs-COOH,CHIT/GCE (curve 3) and aptamer/Comp. Str./MWCNTs-COOH,CHIT/GCE (curve 4). (**B**) CVs of modified electrodes in 0.1 M KCl solution containing 5.0 mM $[Fe(CN)_6]^{3-/4-}$: MWCNTs-COOH,CHIT/GCE (curve 1), Comp. Str./MWCNTs-COOH,CHIT/GCE (curve 2) and aptamer/Comp. Str./MWCNTs-COOH,CHIT/GCE (curve 3). (**C**) CVs of modified electrodes in 0.1 M PBS (pH 7) at a scan rate of 0.1 V/s: bare GCE (curve 1), MWCNTs-COOH,CHIT/GCE (curve 2), aptamer/Comp. Str./MWCNTs-COOH,CHIT/GCE (curve 3) and BPA/aptamer/Comp. Str./MWCNTs-COOH,CHIT/GCE (curve 4).

In addition, to demonstrate the possibility of this process, the electrochemical behaviors of the aptasensor were observed using CV after each step in PBS (pH 7) (figure 2C). Upon Fc-aptamer introduction, a pair of clear redox peaks at 0.02 and 0.55 V (vs Ag/AgCl) appeared at 0.1 V/s (curve 3). More favorably, the peak currents diminished upon adding BPA (curve 4), which was principally attributed to the detachment of the Fc-aptamer from the electrode. Moreover, a specific platform was provided for amplified aptamer loading through interactions with covalent immobilized Comp. Str.

3.3 *Optimization of experimental conditions*

In detail, two important factors were considered to be optimized: the amount of aptamer and Comp. Str. and the incubation time for aptamer and BPA interaction. As can be seen in figure 3, the oxidation current increased with the aptamer amounts up to ~8 μL of 100 μM and then plateaued. Due to the surface saturation, it was observed that the current reduced after an increase in the volumes according to the literature (Beiranvand *et al.* 2017; He and Yan 2018). Thus, 8 μL of aptamer (100 μM) was used as the optimal amount. The other important factor is the incubation time for the aptamer to capture BPA and affect the detection range. As shown in figure 4, by increasing the incubation time, the oxidation current first quickly decreased and remained steady at about 60 min which indicates sufficient time period for complete interaction between BPA and its aptamer; this time was selected to examine the effect of the scan rate, calibration test and so on.

3.4 *Investigation of the scan rate effect on BPA/aptamer/Comp. Str./MWCNTs-COOH, CHIT/GCE*

To conclude the electrochemical mechanism of the aptasensor, the scan rate effect on the BPA redox reaction was examined.

According to figure 5A, the CV responses to BPA/aptamer/Comp. Str./MWCNTs-COOH,CHIT/GCE were recorded in PBS at various scan rates. By enhancing the scan rate from 0.02 to 0.35 V/s, the redox peak currents regularly increased. The redox peak currents are related to the functional scan rate (figure 5B and C), demonstrating that the process is diffusion controlled. Also, this shows the effective BPA recognition using the fabricated aptasensor. Moreover, when the scan rates were increased, the anodic potential moved to more positive potentials. It suggests that the mechanism of the aptasensor is a quasi-reversible electron transfer (Bard and Faulkner 1980). As shown in figure 4D, the scan rate effect was examined based on the change in cathodic (E_p^c) and anodic (E_p^a) peak potentials vs the logarithm of the scan rate (log v). The effect of the scan rate on E_p^a was investigated via the Laviron equation (Laviron 1979):

$$E_p^a = E^{0'} - \frac{2.3RT}{(1-\alpha)nF}\log\frac{(1-\alpha)Fn\vartheta}{RTk} \quad (2)$$

$$\log k_s = \alpha\log(1-\alpha) + (1-\alpha)\log\alpha - \log\frac{RT}{nF\vartheta} - \frac{\alpha(1-\alpha)Fn\Delta E_p}{2.3RT} \quad (3)$$

where temperature, gas and Faraday constant are indicated by T, R and F, respectively; α, n and k_s are the electron-transfer coefficient, the number of electrons and heterogeneous electron-transfer rate constant, respectively. Assuming $0.3 < \alpha < 0.7$ as usual (Nazari *et al.* 2015; Rafipour *et al.* 2017), it could be resolved that n and α equal to 1 and 0.66, respectively. Thus, the reaction of the aptasensor is one electron-transfer path. Besides, the k_s was obtained to be 0.12/s (table 1).

3.5 *Linear range and detection limit*

The modified electrode was used to determine various BPA concentrations in PBS (pH 7, 0.1 M). According to figure 6A,

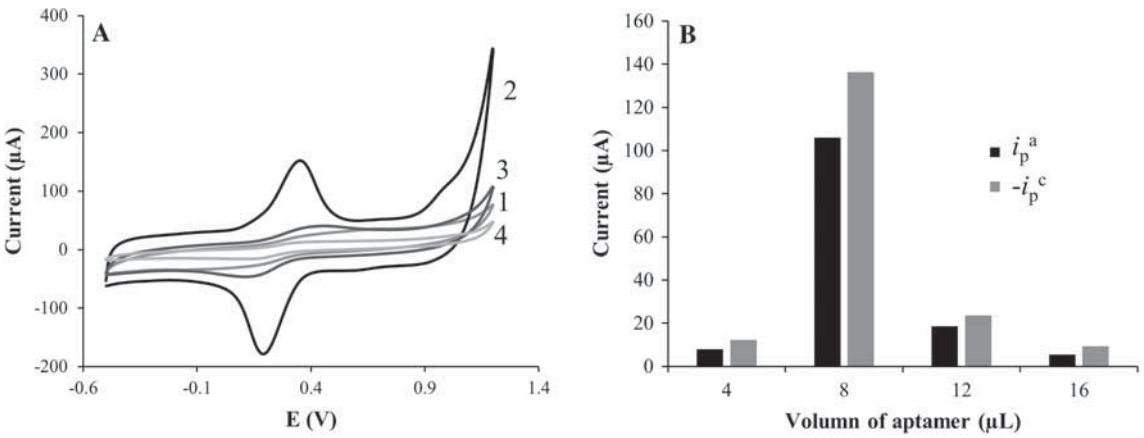

Figure 3. Optimization of aptamer volume in 0.1 M PBS (pH 7) at a scan rate of 0.1 V/s: (**A**) CV curves: 4 μL (curve 1), 8 μL (curve 2), 12 μL (curve 3) and 16 μL (curve 4). (**B**) Bar chart of peak currents vs aptamer volumes.

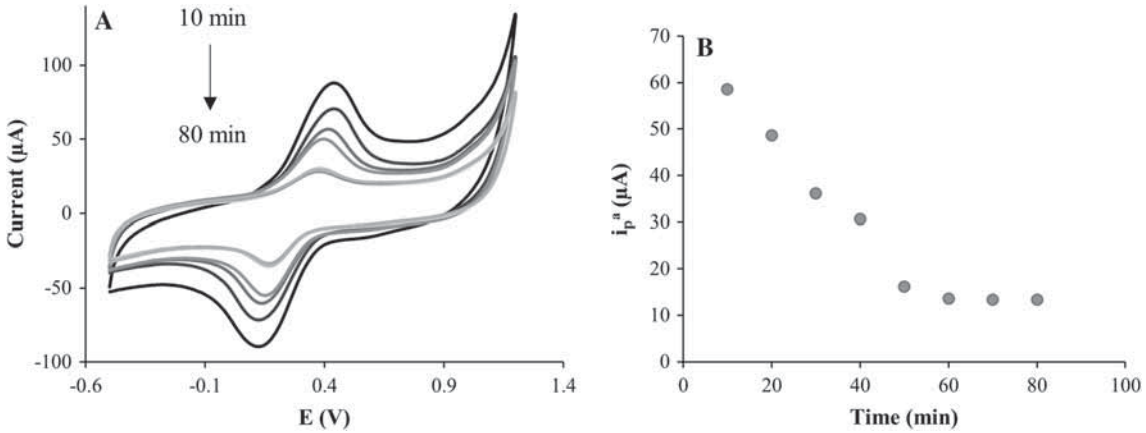

Figure 4. Optimization of incubation time between aptamer and BPA in 0.1 M PBS (pH 7) at a scan rate of 0.1 V/s: (**A**) CV curves and (**B**) linear plot of peak currents vs time incubation.

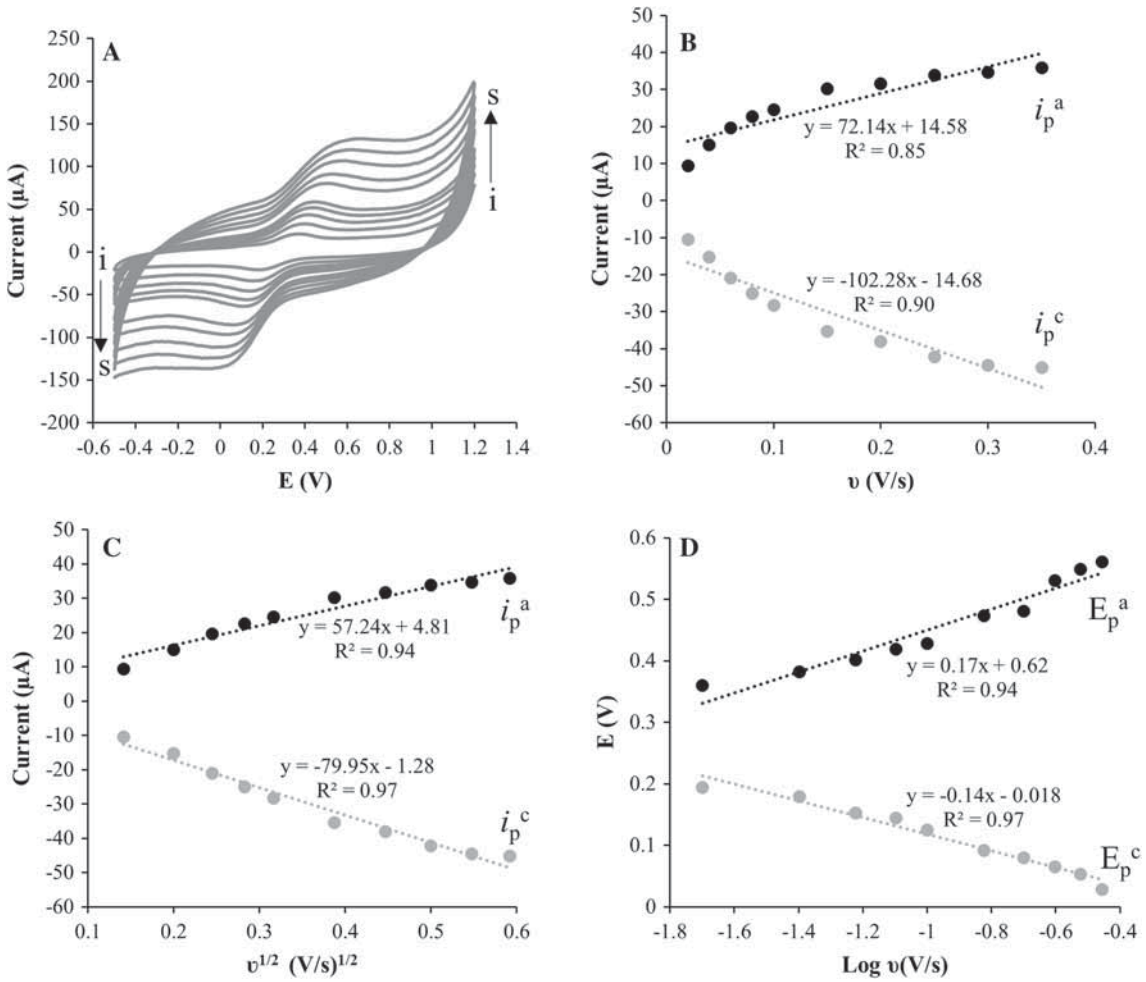

Figure 5. (**A**) Cyclic voltammograms of BPA/aptamer/Comp. Str./MWCNTs-COOH,CHIT/GCE in 0.1 M PBS pH 7.0 at different scan rates. Scan rates from (i) to (s) are 0.02, 0.04, 0.06, 0.08, 0.1, 0.15, 0.2, 0.25, 0.3 and 0.35 V/s. (**B**) The effect of scan rate on anodic and cathodic currents vs the scan rate. (**C**) The effect of scan rate on anodic and cathodic currents vs the square of the scan rate. (**D**) Dependence of peak potentials vs the logarithm of the scan rate.

the DPV peaks of Fc oxidation decrease with an increase in BPA concentration. Figure 6 shows the relationship between the oxidation peak currents of the Fc-labeled aptamer and BPA concentration ranging from 0.2 to 2 nM. The equation is $y = 2.2219 + 24.507C_{BPA}$ ($R^2 = 0.995$), and the LOD is obtained to be 0.38 nM (based on S/N = 3).

Table 1. Cyclic voltammogram information of various scan rates in 0.1 M PBS pH 7.0

Scan rate (V/s)	i_p^a (μA)	E_p^a (V)	i_p^c (μA)	E_p^c (V)
0.02	9.459	0.36	−10.46	0.194
0.04	14.99	0.382	−15.32	0.179
0.06	19.66	0.401	−20.98	0.153
0.08	22.63	0.419	−25.01	0.144
0.1	24.52	0.428	−28.32	0.125
0.15	30.22	0.473	−35.34	0.092
0.2	31.63	0.481	−38.06	0.08
0.25	33.92	0.53	−42.2	0.065
0.3	34.7	0.549	−44.43	0.053
0.35	35.85	0.561	−45.18	0.028

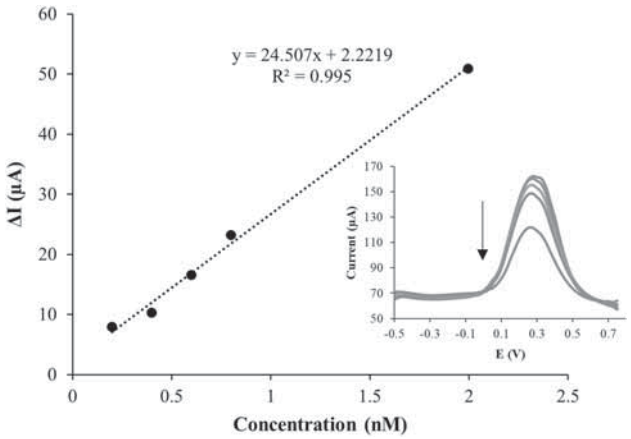

Figure 6. Plot of oxidation peak current vs BPA concentrations. Inset: DPV curves obtained for the proposed aptasensor recorded in 0.1 M PBS solution after incubation with different concentrations of BPA (from a to i): 0.2–2 nM.

3.6 *Reproducibility, repeatability, stability and selectivity of the aptasensor*

For checking the aptasensor reproducibility, three electrodes were used for the fabrication of the proposed aptasensor. The relative standard deviation (RSD) was found to be 3.3% indicating the satisfactory value of reproducibility for the aptasensor. The repeatability of the proposed aptasensor was estimated as well; to this end, six successive current signals were recorded and the RSD was calculated to be 2.99%, which is an acceptable value according to table 2. Also, the stability of the proposed aptasensor was investigated; the RSDs of 95.16 and 83.64% were obtained after 2 weeks and 2 months, respectively.

The selectivity of the proposed aptasensor for BPA was studied under optimal experimental conditions in the phosphate buffer solution containing BPA (1 nM) and the control molecules, including estradiol, progesterone and testosterone, which were structurally analogous to BPA (figure 7) were added to the serum samples.

Table 2. BPA determination in serum samples

Sample	The concentration of spiked BPA (nM)	Detected BPA concentration (nM)	Recovery (%)
1	0.400	0.338	84.53
2	0.799	0.705	88.20

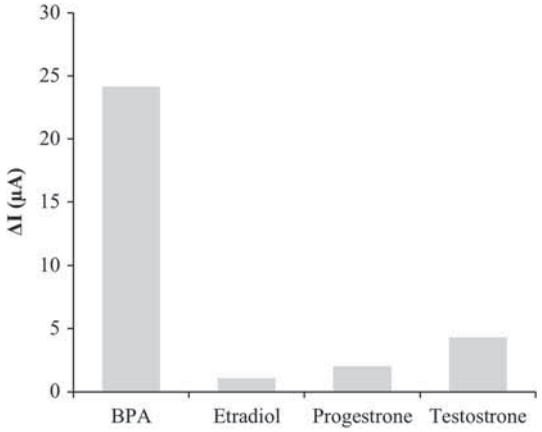

Figure 7. Aptasensor selectivity to BPA molecules and some interference including testosterone, estradiol and progesterone.

3.7 *Real sample analysis*

The recovery test of the aptasensor was evaluated in serum samples for practical applications. According to the literature (Zhu *et al.* 2015), serum samples are rarely used as real samples for BPA detection, while the controlling of BPA concentration should be conformed in clinical samples such as serum to investigate BPA harmful effects. The serum sample was diluted 20 times using PBS; after that it was spiked with various BPA concentrations. The recoveries were obtained as 84.53 and 88.20% (table 2).

4. Discussion

A new redox probe Fc-labeled aptasensor was proposed for BPA detection in this work. The approach was based on the immobilization of Comp. Str. sequence by EDC/NHS chemistry on the electrode surface, the hybridization of an aptamer with immobilized Comp. Str. and the dehybridization of an aptamer in the presence of BPA. According to the FESEM images, the MWCNTs-COOH/CHIT modified with Comp. Str. and Comp. Str./aptamer exhibited denser and more crowded compared with unmodified MWCNTs/CHIT. They were homogeneously distributed on the GCE-modified surface with no agglomeration.

EIS data demonstrate that the coverage of Comp. Str. diminished the electrode surface area and delayed the probe electron transferring ($[Fe(CN)_6]^{3-/4-}$); thus it causes increase of the R_{et} value for Comp. Str./MWCNTs-COOH,CHIT/

GCE. As can be seen, the R_{et} value of the aptamer/Comp. Str./MWCNTs-COOH,CHIT/GCE is less than that of Comp. Str./MWCNTs-COOH,CHIT/GCE due to the presence of the Fc group in the 5′ tail of the aptamer. A palindrome sequence of eight base pairs was selected at the ends of Comp. Str. to provide a hair pin shape in the absence of the BPA aptamer. Hence, by its immobilization on the electrode surface, Comp. Str. can form a loop-stem structure. In the absence of BPA, Comp. Str. hybridizes with the Fc-labeled aptamer which keeps the Fc group near to the surface of the electrode, therefore an electrochemical signal can be obtained.

Cyclic voltammograms confirm the enhancement of the electrode conductivity and facilitate the electron transfer due to the presence of MWCNTs-COOH on the electrode surface. After immobilization of Comp. Str. (Comp. Str./MWCNTs-COOH,CHIT/GCE), redox currents have reduced, because $[Fe(CN)_6]^{3-/4-}$ and Comp. Str. have similar charges, causing electrostatic repulsion. Nevertheless, strong peak currents can be observed for the aptamer/Comp. Str./MWCNTs-COOH,CHIT/GCE because of the specific and strong integration between the BPA aptamer and Comp. Str. and the presence of the Fc group in the 5′ tail of the aptamer. After incubation (for 60 min) of the aptasensor with 1 μM BPA, the redox currents greatly decreased, which approves the strong interaction between the aptamer and the BPA, due to the aptamer/Comp. Str. duplex dissociation and release of the aptamer from the surface of the electrode, due to the higher affinity of BPA and its aptamer compared with the aptamer and the Comp. Str. Also, the calculated large surface area of the proposed aptasensor confirms the presence of the Fc group of the functionalized BPA aptamer. After the aptamer attachment to the modified GCE, the potential difference decreased and the redox currents increased, representing the Fc-labeled aptamer coverage at the modified-electrode surface and retarded the improved electron transferring. The aptasensor incubation with 1 μM BPA causes aptamer conformational changes upon BPA binding and more delay in the interfacial electron exchange; consequently, for the aptasensor a considerable electrochemical signal decrease was detected.

The results of EIS and CV measurements were consistent with each other and clearly confirmed the fabrication of the aptasensor. These results revealed that this BPA aptasensor can be used for BPA monitoring.

Under optimal conditions, the modified electrode displayed high sensitivity and low LOD. Compared with the other BPA sensors and the indicated biosensors in table 3, the proposed aptasensor demonstrates more sensitivity for the BPA detection (Deiminiat *et al.* 2017) and lower detection limit (Huang *et al.* 2011; Yang *et al.* 2014; Zhou *et al.* 2014; Goulart *et al.* 2016). In addition, in table 3, the stability of some BPA biosensors is reported; as can be seen, the proposed aptasensor has good stability after 2 weeks when compared with the others.

The specificity of the developed aptasensor was studied in the presence of human hormones having a similar structure

Table 3. Comparison of different electrodes for BPA detection in solutions

Method	Linear range	LOD (nM)	Sensitivity (μA/nM)	Stability (RSD% for 2 weeks)	Reproducibility (RSD%)	Repeatability (RSD%)	Ref.
Peptide/Au electrode	1–5000 nM	0.7	–	–	7.6	–	Yang *et al.* (2014)
f-MWCNTs/AuNPs nanocomposite/aptasensor	0.1–10 nM	0.05	3.2356	94	3.5	–	Deiminiat *et al.* (2017)
Aptamer/Fe_3O_4/AuNPs/CNTs/GCE	1–20, 50–600 nM	0.3	–	92	6.1	–	Beiranvand and Azadbakht (2017)
Aptamer/AuNPs/GR/GCE	0.01–10 μM	5	–	~95	3.2	–	Zhou *et al.* (2014)
Sol–gel MIP/GNPs/MWCNTs/Au	0.113–8.21 μM	3.6	–	–	–	4.8	Huang *et al.* (2011)
MWCNTs/GCE	2.5–29.1 μM	0.61 μM	31.3	–	–	–	Goulart *et al.* (2016)
MCH/aptamer/Fe_3O_4-SH@Au/MWCNT/GCE	0.1–8 nM	0.03	86.43 μA/nM cm^2	95.3 (for 1 week)	4.4	–	Baghayeri *et al.* (2018)
Aptamer/Comp. Str./MWCNTs-COOH,CHIT/GCE	0.2–2 nM	0.38	24.507	95.16	3.3	2.99	This work

f-MWCNTs, functionalized multiwalled carbon nanotubes; AuNPs, gold nanoparticles; GR, graphene.

to BPA. As is shown, only BPA caused a decrease in the current response, while no current changes were observed in the presence of other interference with the concentration 10 times greater than that of BPA, indicating that the proposed aptasensor has an acceptable specificity toward BPA in the presence of similar molecules which may exist in serum.

Also, it was used for the BPA determination in serum samples with the recovery results being obtained. The results indicate that this aptasensor is acceptable and practicable in order to apply in real sample analysis. This design can be applied to fabricate aptasensors for the detection of other analyte molecules.

References

Baghayeri M, Ansari R, Nodehi M, Razavipanah I and Veisi H 2018 Voltammetric aptasensor for bisphenol A based on the use of a MWCNT/Fe_3O_4@gold nanocomposite. *Microchim. Acta* **185** 320–329

Bard A and Faulkner L 1980 *Electrochemical methods fundamentals and applications* (New York: Wiley)

Beiranvand S and Azadbakht A 2017 Electrochemical switching with a DNA aptamer-based electrochemical sensor. *Mater. Sci. Eng. C* **76** 925–933

Beiranvand ZS, Abbasi AR, Dehdashtian S, Karimi Z and Azadbakht A 2017 Aptamer-based electrochemical biosensor by using Au–Pt nanoparticles, carbon nanotubes and acriflavine platform. *Anal. Biochem.* **518** 35–45

Cao W, Chao Y, Liu L, Liu Q and Pei M 2014 Flow injection chemiluminescence sensor based on magnetic oil-based surface molecularly imprinted nanoparticles for determination of bisphenol A. *Sens. Actuators B* **204** 704–709

Cunha S, Pena A and Fernandes J 2015 Dispersive liquid–liquid microextraction followed by microwave-assisted silylation and gas chromatography-mass spectrometry analysis for simultaneous trace quantification of bisphenol A and 13 ultraviolet filters in wastewaters. *J. Chromatogr. A* **1414** 10–21

Darmostuk M, Rimpelova S, Gbelcova H and Ruml T 2015 Current approaches in SELEX: an update to aptamer selection technology. *Biotechnol. Adv.* **33** 1141–1161

Deiminiat B, Rounaghi GH, Arbab-Zavar MH and Razavipanah I 2017 A novel electrochemical aptasensor based on f-MWCNTs/AuNPs nanocomposite for label-free detection of bisphenol A. *Sens. Actuators B* **242** 158–166

European Food Safety Authority (EFSA) 2015 Scientific opinion on the risks to public health related to the presence of bisphenol A (BPA) in foodstuffs: executive summary. *EFSA J.* **13** 3978–5018

Farajzadeh MA, Abbaspour M, Mogaddam MRA and Ghorbanpour H 2015 Determination of some synthetic phenolic antioxidants and bisphenol A in honey using dispersive liquid–liquid microextraction followed by gas chromatography-flame ionization detection. *Food Anal. Methods* **8** 2035–2043

Feng J, Xu L, Cui G, Wu X, Ma W, Kuang H and Xu C 2016 Building SERS-active heteroassemblies for ultrasensitive bisphenol A detection. *Biosens. Bioelectron.* **81** 138–142

Filippou O, Deliyanni EA and Samanidou VF 2017 Fabrication and evaluation of magnetic activated carbon as adsorbent for ultrasonic assisted magnetic solid phase dispersive extraction of bisphenol A from milk prior to high performance liquid chromatographic analysis with ultraviolet detection. *J. Chromatogr. A* **1479** 20–31

Goulart LA, de Moraes FC and Mascaro H 2016 Influence of the different carbon nanotubes on the development of electrochemical sensors for bisphenol A. *Mater. Sci. Eng. C* **58** 768–773

He B-S and Yan S 2018 Electrochemical aptasensor based on aptamer-complimentary strand conjugate and thionine for sensitive detection of tetracycline with multiwalled carbon nanotubes and gold nanoparticles amplification. *Anal. Methods* **10** 783–790

He M-Q, Wang K, Wang J, Yu Y-L and He R-H 2017 A sensitive aptasensor based on molybdenum carbide nanotubes and label-free aptamer for detection of bisphenol A. *Anal. Bioanal. Chem.* **409** 1797–1803

Huang J, Zhang X, Lin Q, He X, Xing X, Huai H, Lian W and Zhu H 2011 Electrochemical sensor based on imprinted sol–gel and nanomaterials for sensitive determination of bisphenol A. *Food Control* **22** 786–791

Huang R, Xi Z and He N 2015 Applications of aptamers for chemistry analysis, medicine and food security. *Sci. China Chem.* **58** 1122–1130

Jo M, Ahn J-Y, Lee J, Lee S, Hong SW, Yoo J-W, Kang J, Dua P, Lee D-K and Hong S 2011 Development of single-stranded DNA aptamers for specific bisphenol A detection. *Oligonucleotides* **21** 85–91

Kazane I, Gorgy K, Gondran C, Spinelli N, Zazoua A, Defrancq E and Cosnier S 2016 Highly sensitive bisphenol-A electrochemical aptasensor based on poly(pyrrole-nitrilotriacetic acid)-aptamer film. *Anal. Chem.* **88** 7268–7273

Kubo I, Kanamatsu T and Furutani S 2014 Microfluidic device for enzyme-linked immunosorbent assay (ELISA) and its application to bisphenol A sensing. *Sens. Mater.* **26** 615–621

Laviron E 1979 General expression of the linear potential sweep voltammogram in the case of diffusionless electrochemical systems. J. Electroanal. Chem. *Interfacial Electrochem.* **10** 19–28

Liu G, Chen Z, Jiang X, Feng D-Q, Zhao J, Fan D and Wang W 2016 In-situ hydrothermal synthesis of molecularly imprinted polymers coated carbon dots for fluorescent detection of bisphenol A. *Sens. Actuators B* **228** 302–307

Lv E, Ding J and Qin W 2018 Potentiometric aptasensing of small molecules based on surface charge change. *Sens. Actuators B* **259** 463–466

Ma Y, Liu J and Li H 2017 Diamond-based electrochemical aptasensor realizing a femtomolar detection limit of bisphenol A. *Biosens. Bioelectron.* **92** 21–25

Maiolini E, Ferri E, Pitasi AL, Montoya A, Di Giovanni M, Errani E and Girotti S 2014 Bisphenol A determination in baby bottles by chemiluminescence enzyme-linked immunosorbent assay, lateral flow immunoassay and liquid chromatography tandem mass spectrometry. *Analyst* **139** 318–324

Mei Z, Chu H, Chen W, Xue F, Liu J, Xu H, Zhang R and Zheng L 2013 Ultrasensitive one-step rapid visual detection of bisphenol A in water samples by label-free aptasensor. *Biosens. Bioelectron.* **39** 26–30

Miao W, Wei B, Yang R, Wu C, Lou D, Jiang W and Zhou Z 2014 Highly specific and sensitive detection of bisphenol A in water

samples using an enzyme-linked immunosorbent assay employing a novel synthetic antigen. *New J. Chem.* **38** 669–675

Nazari M, Kashanian S and Rafipour R 2015 Laccase immobilization on the electrode surface to design a biosensor for the detection of phenolic compound such as catechol. Spectrochim. *Acta Part A* **145** 130–138

Ohkuma H, Abe K, Ito M, Kokado A, Kambegawa A and Maeda M 2002 Development of a highly sensitive enzyme-linked immunosorbent assay for bisphenol A in serum. *Analyst* **127** 93–97

Peng X, Kang L, Pang F, Li H, Luo R, Luo X and Sun F 2018 A signal-enhanced lateral flow strip biosensor for ultrasensitive and on-site detection of bisphenol A. *Food Agric. Immunol.* **29** 1–12

Rafipour R, Kashanian S, Hashemi S, Omidfar K and Ezzati Nazhad Dolatabadi J 2017 Apoferritin-templated biosynthesis of manganese nanoparticles and investigation of direct electron transfer of MnNPs-HsAFr at modified glassy carbon electrode. *Biotechnol. Appl. Biochem.* **64** 110–116

Rocha BA, da Costa BRB, de Albuquerque NCP, de Oliveira ARM, Souza JMO, Al-Tameemi M, Campiglia AD and Barbosa F Jr 2016 A fast method for bisphenol A and six analogues (S, F, Z, P, AF, AP) determination in urine samples based on dispersive liquid–liquid microextraction and liquid chromatography-tandem mass spectrometry. *Talanta* **154** 511–519

Salehi AS, Yang SO, Earl CC, Tang MJS, Hunt JP, Smith MT, Wood DW and Bundy BC 2018 Biosensing estrogenic endocrine disruptors in human blood and urine: A RAPID cell-free protein synthesis approach. *Toxicol. Appl. Pharmacol.* **345** 19–25

Sekar TV, Foygel K, Massoud TF, Gambhir SS and Paulmurugan R 2016 A transgenic mouse model expressing an ERα folding biosensor reveals the effects of bisphenol A on estrogen receptor signaling. *Sci. Rep.* **6** 34788

Sheikh IA, Tayubi IA, Ahmad E, Ganaie MA, Bajouh OS, AlBasri SF, Abdulkarim IM and Beg MA 2017 Computational insights into the molecular interactions of environmental xenoestrogens 4-tert-octylphenol, 4-nonylphenol, bisphenol A (BPA), and BPA metabolite, 4-methyl-2,4-bis(4-hydroxyphenyl)pent-1-ene (MBP) with human sex hormone-binding globulin. *Ecotoxicol. Environ. Saf.* **135** 284–291

Steinmetz R, Brown NG, Allen DL, Bigsby RM and Ben-Jonathan N 1997 The environmental estrogen bisphenol A stimulates prolactin release in vitro and in vivo. *Endocrinology* **138** 1780–1786

U. S. Food and Drug Administration 2014 Bisphenol A (BPA): use in food contact application, FDA

Wang X, Reisberg S, Serradji N, Anquetin G, Pham M-C, Wu W, Dong C-Z and Piro B 2014 E-assay concept: detection of bisphenol A with a label-free electrochemical competitive immunoassay. *Biosens. Bioelectron.* **53** 214–219

Xue F, Wu J, Chu H, Mei Z, Ye Y, Liu J, Zhang R, Peng C, Zheng L and Chen W 2013 Electrochemical aptasensor for the determination of bisphenol A in drinking water. *Microchim. Acta* **180** 109–115

Yan K, Yang Y and Zhang J 2018 A self-powered sensor based on molecularly imprinted polymer-coupled graphitic carbon nitride photoanode for selective detection of bisphenol A. *Sens. Actuators B* **259** 394–401

Yang J, Kim S-E, Cho M, Yoo I-K, Choe W-S and Lee Y 2014 Highly sensitive and selective determination of bisphenol-A using peptide-modified gold electrode. *Biosens. Bioelectron.* **61** 38–44

Yu P, Liu Y, Zhang X, Zhou J, Xiong E, Li X and Chen J 2016 A novel electrochemical aptasensor for bisphenol A assay based on triple-signaling strategy. *Biosens. Bioelectron.* **79** 22–28

Zehani N, Fortgang P, Lachgar MS, Baraket A, Arab M, Dzyadevych SV, Kherrat R and Jaffrezic-Renault N 2015 Highly sensitive electrochemical biosensor for bisphenol A detection based on a diazonium-functionalized boron-doped diamond electrode modified with a multi-walled carbon nanotube-tyrosinase hybrid film. *Biosens. Bioelectron.* **74** 830–835

Zhang D, Yang J, Ye J, Xu L, Xu H, Zhan S, Xia B and Wang L 2016 Colorimetric detection of bisphenol A based on unmodified aptamer and cationic polymer aggregated gold nanoparticles. *Anal. Biochem.* **499** 51–56

Zhou L, Wang J, Li D and Li Y 2014 An electrochemical aptasensor based on gold nanoparticles dotted graphene modified glassy carbon electrode for label-free detection of bisphenol A in milk samples. *Food Chem.* **162** 34–40

Zhou L, Jiang D, Du X, Chen D, Qian J, Liu Q, Hao N and Wang K 2016 Femtomolar sensitivity of bisphenol A photoelectrochemical aptasensor induced by visible light-driven TiO_2 nanoparticle-decorated nitrogen-doped graphene. *J. Mater. Chem. B* **4** 6249–6257

Zhu Y, Zhou C, Yan X, Yan Y and Wang Q 2015 Aptamer-functionalized nanoporous gold film for high-performance direct electrochemical detection of bisphenol A in human serum. *Anal. Chim. Acta* **883** 81–89

Zimmers SM, Browne EP, O'Keefe PW, Anderton DL, Kramer L, Reckhow DA and Arcaro KF 2014 Determination of free bisphenol A (BPA) concentrations in breast milk of US women using a sensitive LC/MS/MS method. *Chemosphere* **104** 237–243

Corresponding editor: BJ Rao